JOURNAL OF MATERIALS SCIENCE: MATERIALS IN MEDICINE 4 (1993) 460–465

The crystallization behavior of gallstones grown from cholesterol

S. KUMAR, S. J. BURNS*
Materials Science Program, Department of Mechanical Engineering, University of Rochester, Rochester, NY 14627-0133, USA

Cholesterol is the major crystalline component of most gallstones found in the western hemisphere. Synthetic gallstones have been grown in our laboratory from cholesterol to study both growth morphology and kinetics. It is established that synthetic stones show characteristics of spherulitic crystallization. It is suggested that natural stones *in vivo* will also crystallize by spherulitic mechanisms. The microstructure of synthetic and natural stones consists of radiating arrays of cholesterol crystals emerging from a unique nucleation center. Impurities which are used to thicken the melt are segregated between the fibers. The radial growth of these fibers was observed to be a linear function of time. The radial growth rates are reported over a range of temperatures for support of a spherulitic model.

1. Introduction

Gallstone is a misnomer; they are not ceramic stones but are generally organic concretions formed in the gall bladder or biliary passages. Gallstones may be classified according to their composition as cholesterol-rich, mixed or pigment stones. Cholesterol is the major constituent of almost all gallstones found in the western hemisphere [1]. It has been reported that the cholesterol composition is as high as 95–98% in certain cases. The other components frequently reported are calcium bilirubinate, calcium carbonate and bile pigments [2, 3].

Attempts have been made to understand the formation of gallstones from the natural bile solution that is found in the gall bladder [4, 5]. Despite intensive research work, the understanding of cholesterol gallstone formation has remained fragmentary and incomplete. An understanding of the nucleation and growth of gallstones could lead to immediate benefits: a high nucleation rate might result in the formation of small stones that can be passed by the bile duct; growth inhibitors could be used to suppress formation of large stones. Either process would be non-invasive and would avoid cholesystectomies, which are surgical gall bladder removals. The role of calcium salts, pigments, etc., is not well understood in nucleation of these stones, although cholesterol stones are reported to contain a pigment center [6]. In this study, gallstones have been grown from cholesterol solutions and from a melt to study their crystallization behavior. The growth morphology of the crystals and spherulitic crystallization kinetics are reported. Here we have also shown that the synthetic stones which we have made very closely resemble the spherlitic crystallization of polymers from the melt and the crystallographic morphology of natural stones that have been cut and polished. The microstructure of our synthetic stones and of natural stones are practically indistinguishable. Finally, we report on several of the mechanical properties of our synthetic stones.

2. Differential scanning calorimetry (DSC)

The thermal properties of cholesterol were measured using DSC. The cholesterol powder had a purity of 95% and was purchased commercially (Sigma Co.). The DSC was previously calibrated using an indium reference standard. The rate of heating was 20 °C min^{-1} and the rate of cooling was 3 °C min^{-1}. The DSC thermographs are shown in Fig. 1. The melting point is 149.8 °C, which is essentially the published value of 149 °C that is reported in the literature [7]. The measured freezing point is 121.1 °C, thus a supercooling of about 29 °C was achieved before recrystallization started in this sample. The heat of fusion is 27.1 kJ mol^{-1}, while the heat of recrystallization is 21.4 kJ mol^{-1}.

3. Growth morphology

Crystallization of cholesterol was studied from the melt in several different ways. The simplest method was to test a small amount of cholesterol powder by sprinkling it on a microscope slide. The slide was then placed on a hot plate and the cholesterol was allowed to melt. On subsequent melting the solid was covered with an optical cover slip for protection and observation. Finally, the temperature was controlled by very slowly adjusting the hotplate's electrical power. The thin solid film that was deposited on the glass plate was then observed under an optical microscope in

* Author to whom correspondence should be addressed.

0957–4530

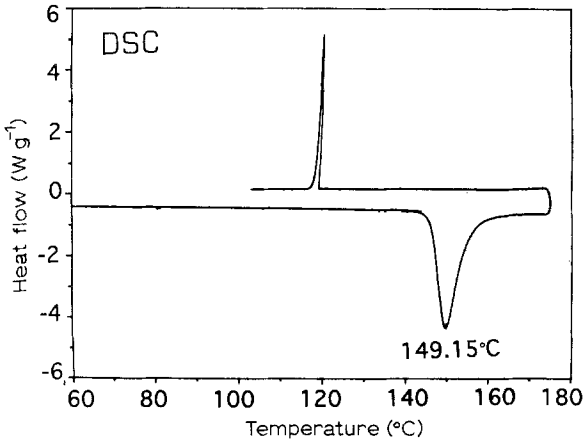

Figure 1 The DSC results for cholesterol (95% purity). The rate of heating was 20 °C min^{-1} and the rate of cooling 3 °C min^{-1}.

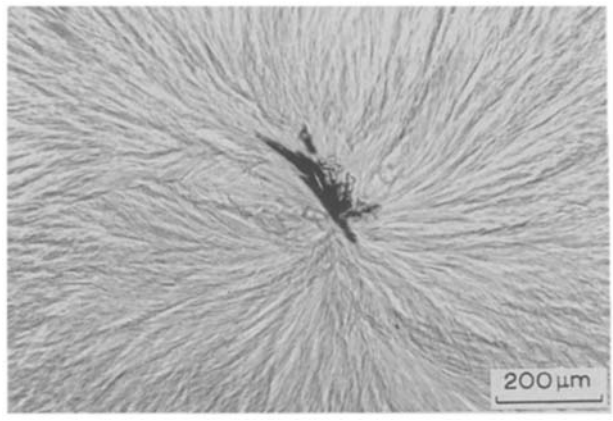

Figure 2 A transmission optical photomicrograph of slowly cooled cholesterol melt on a microscope slide. The stone starts to grow from the nucleus near the center exhibiting spherulitic crystallization.

transmission mode. The structure of this type of film is shown in Fig. 2. There is a centrally located nucleation site from which the radial crystals start to grow. This growth pattern is a characteristic of spherulitic crystallization, widely observed in polymers crystallizing from the melt [8, 9]. In spherulitic crystallization the primary nucleus initiates the growth not of a single crystal, but of a polycrystalline aggregate which consists of radiating arrays of fine crystalline fibers emanating from one center. The individual aggregates are called spherulites. The outward growth of a spherulite ceases when it has impinged upon the growing surface of another spherulite. In Fig. 2 we also observe splitting of the fibers at very small angles. This is called non-crystallographic branching or small angle branching [8] between the parent and daughter crystallites.

The physics of spherulitic growth have been investigated by Keith and Padden [8], who explained their results in terms of constitutional supercooling. Under spherulitic conditions small projections can form at the solid–liquid interface, these projections, moreover, remain stable during subsequent growth, resulting in radial or spherulitic behavior. The DSC results indicate the very large amount of supercooling that cholesterol undergoes. Impurities in spherulitic crystallization contribute to constitutional supercooling of the melt and can change the viscosity of the melt as thickeners. These impurities are rejected at the growth front interface and subsequently are trapped between the expanding fibers. In the present case, calcium salts are present as impurities. They act as thickeners and will increase melt viscocity. In a previous study on natural gallstone microstructures, it was found that cholesterol and calcium bilirubinate occurred as adjacent layers [6]. During the spherulitic growth of cholesterol, calcium bilirubinate should have segregated between the fibers. Pigments could act as nucleation sites and be present at the gallstone center, as has been suggested before [6]. In more recent work, the presence of chiral twins in the radial cholesterol crystals has been reported [10]. Chiral twins have the same physical and chemical properties, but differ in optical rotation; the rotation is by the same magnitude but in opposite directions. Therefore, they have different colors, due to different optical retardations, under a transmission optical microscope. No chiral twinning was observed in the stones grown from synthetic cholesterol.

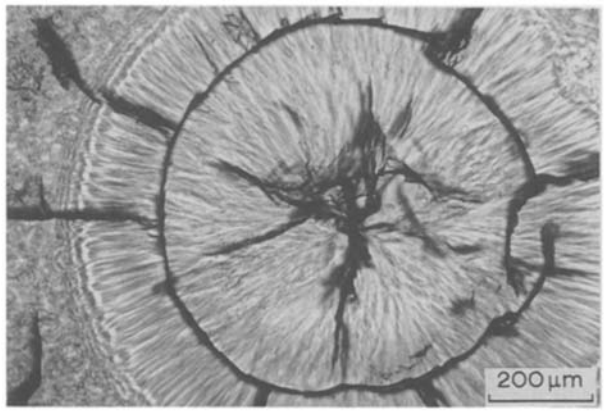

Figure 3 A transmission optical photomicrograph of a quenched sample. Both radial cracks and circular cracks are evident as thin black lines.

In a second experiment a thin melt of cholesterol was quenched to room temperature. This led to the formation of cracks, as shown in Fig. 3. Both radial cracks and circular cracks are present. Natural gallstones also show both circular and radial cracking, especially in dried, polished, thin sections. Some concretions are pulverized inside a patient's body using ultrasonic extracorporeal shock wave lithotripsy (ESWL). The failure mechanism in ESWL is not understood [10] and failure is not very frequent with gallstones. In fragmenting natural gallstones the failure mechanism is a major consideration motivating our study of cholesterol solidification. The flaws in gallstones will determine the strength of the material by providing stress concentrations and by finally propagating as cracks. Fig. 3 has significance in the sense that it shows specific regions of the synthetic stones that easily form flaws. For example, those regions where impurities are rejected from the melt and then collected are prone to being incipient cracks and possibly the "critical flaw" that is needed in a fracture mechanics type of analysis.

4. Growth kinetics

The growth kinetics were measured using cine photography. A porcelain plate with bowl-shaped groves in it was used as a mold. Cholesterol powder (95% purity) was put into the mold and then electrically heated through the porcelain. The temperature of the mold was maintained slightly ($\sim 5\,^{\circ}C$) above the known melting point to completely liquify the cholesterol powder. A photographic camera, fitted with a macro lens, was then focussed on the melt. The temperature of the melt was then very slowly decreased to below the melting point. Fig. 4 is an example where at $133 \pm 1\,^{\circ}C$ a synthetic stone nucleated near the center of the melt. The cine camera was then activated and pictures of the subsequent growth were taken automatically at a rate of 2 frames per second. Two sequential pictures are shown in Fig. 4(a) and (b). The diameters of the synthetic stones during growth were measured and a graph was constructed with the radius of the spherulites on the ordinate and the elapsed time as the abscissa. This plot yielded a straight line, which corresponds to a constant growth rate, which is another characteristic of spherulitic crystallization. Since a few seconds had elapsed subsequent to nucleation but before starting the cine photography, the exact nucleation time could only be estimated by extrapolation from the slope of the graph. A typical growth curve is shown in Fig. 5.

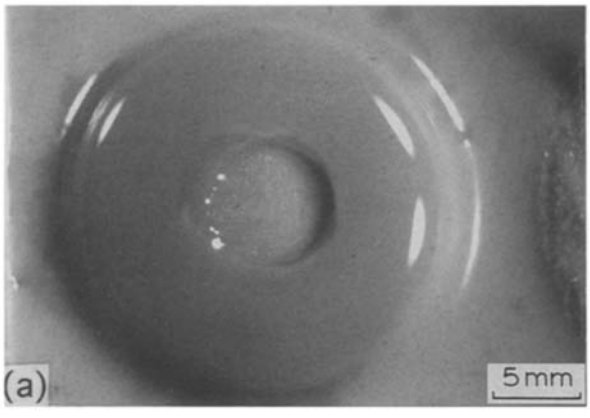

Figure 4(a) A high speed photograph of cholesterol crystallizing from the melt.

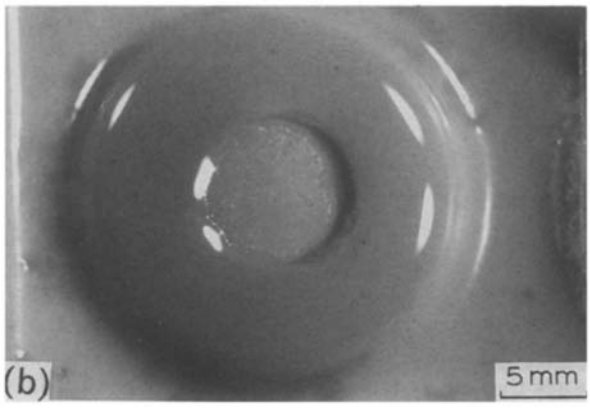

Figure 4(b) The same region of the melt after half a second. The central portion is the stone growing radially in the surrounding melt. The melt is contained in a porcelain mold.

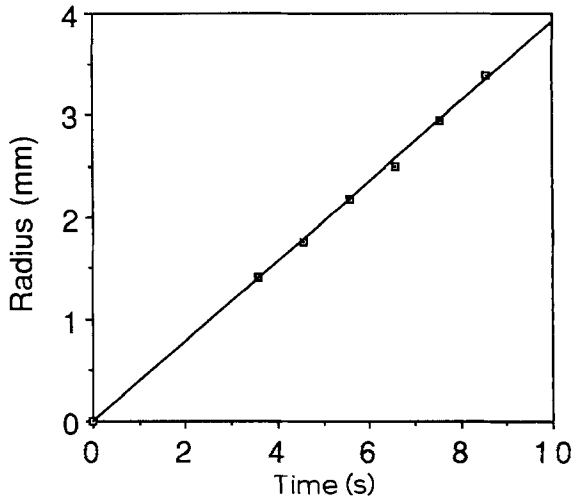

Figure 5 A plot of the measured spherulite radius versus elapsed time for cholesterol (95%). The recrystallization temperature was $133 \pm 1\,^{\circ}C$.

The radial growth rate on an isotherm is independent of time, which is characteristic of spherulitic crystallization [11]. The radial growth rate is $400\,\mu m\,s^{-1}$ at $133\,^{\circ}C$.

The radial growth rates were also measured for cholesterol spherulites grown under a microscope on a hot stage. The pictures were recorded using a video camera mounted on the microscope. However, the cholesterol (95% purity) could not be supercooled below $120\,^{\circ}C$ because nucleation takes place quite easily. The growth rate with 95% purity was too fast for recording kinetic measurements. With cholesterol of 99% purity it was possible to attain much greater supercooling at rates that could be more easily recorded. These radial growth rates as a function of recrystallization temperature are shown in Fig. 6. With increasing supercooling the growth rate increases, reaches a maximum and then decreases again. Similar behavior is reported for spherulitic crystallization of polymers [9, 12]. In the case of polymers it has been established that adding impurities alters the height of the rate peaks, although the peak is attained at the same recrystallization temperature [12]. The radial growth rate as a function of undercooling, reported here in Fig. 6, is not as smooth as comparable curves in polymers [9, 12]. In the case of spherulitic polymers it has been established that with increasing supercooling the growth rate increases, reaches a maximum and decreases again [9, 12]. Similar behavior in growth rate is observed in the case of metals, glasses and ceramics, although they do not exhibit spherulitic growth. In their case any phase transformation is represented as a time-temperature transformation, or TTT curve. The transformation temperature is plotted versus time. Since the growth rate is maximum at intermediate temperature, the transformation time is shortest at this temperature. The transformation time gradually increases at temperatures lower or higher than this.

Fig. 4(a) shows that there is only one nucleation site, which gives rise to a single spherulite. A single nucleation site seems to be dominant for natural gallstones also [6, 10]. Whereas in polymers spherulites are the

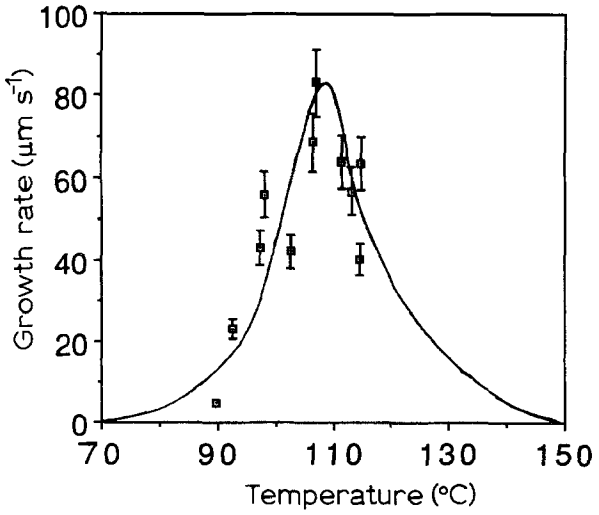

Figure 6 Spherulitic growth rates for cholesterol (99%) as a function of recrystallization temperature.

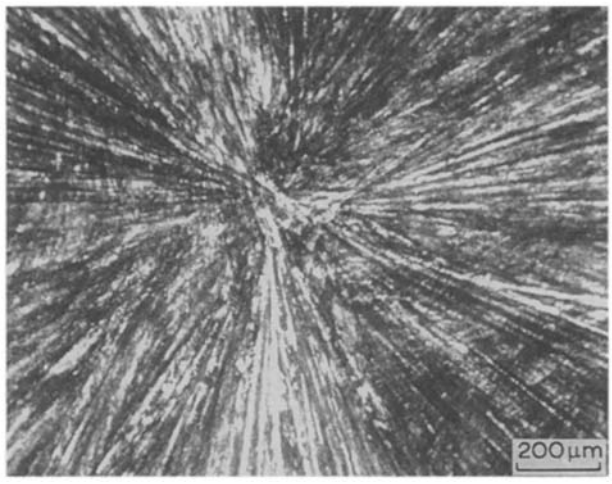

Figure 7 A transmission optical photomicrograph of a stone grown from a supersaturated solution of cholesterol in acetic acid.

metal analog of grains and their size is of the order of microns, natural gallstones as large as a few centimeters in diameter have been observed and they are single spherulites [13].

The study in this paper has been made on gallstones grown from cholesterol melt. Natural gallstones occur presumably as a result of precipitation of cholesterol from a supersaturated bile solution. Cholesterol stones have also been grown in this study from a supersaturated solution of cholesterol in acetic acid. The stones which were grown from solution also resulted in spherulitic crystallization, as shown in Fig. 7. In this latter case the morphology is the same as microstructures grown from the melt, but there are differences in the driving forces and also in the final composition of the stones that are formed.

5. Mechanical characterization: sample preparation

Bar-shaped samples $6 \times 6 \times 25$ mm were prepared by casting cholesterol (95%) in a high precision quartz mold. The cholesterol powder was melted in a beaker at about 160 °C, then cast in the molds. The melt itself does not crystallize unless it is supercooled to between 125 °C and 130 °C, as the DSC results have shown. Crystallization at this temperature yields smooth samples with a very fine microstructure. It can also be crystallized near its melting point by dropping a "seed crystal" of cholesterol into the melt. In this case the growth rate is slow and the resulting microstructure is quite coarse. Spherulitic fibers as thick as 1 mm can easily be grown. A common problem associated with sample preparation was bending and cracking of the bars. Cracking seems to occur due to the difference in the thermal expansion coefficients of the quartz mold and the cast cholesterol.

Natural gallstones when exposed to the atmosphere also develop cracks. However, in this latter case the cracks result from loss of water. Therefore, after fabrication the samples were kept submerged in water. Even with this precaution, some samples still cracked before any mechanical testing. The other problem encountered during casting was coring, which results from the fact that the melt density is less than the solid density. Sometimes a bubble escaping from the bottom of the mold rises to the top leaving a hole running throughout the length of the sample. These two problems were solved by maintaining the thermal gradients such that the crystal nucleates at the bottom of the mold and the interface gradually crystallizes toward the top. With this method coring was confined to the very top portion of the sample. The ends of the sample which are the loading faces were polished with 240 grit SiC paper before mechanical testing. The resulting microstructure was such that the spherulitic fibers were running almost completely parallel or at a very small angle to the axial length of the sample.

6. Stress–strain curves

Melt cast bars were tested on a screw-driven universal testing machine. Owing to the brittle nature of the material, it was tested in compression. The size of the test specimen was 24 mm in length and 6 mm by 6 mm in cross-section. A cross-head speed of 0.01 mm s^{-1} was used. An extensometer with knife edges was mounted on the sample. Although care was taken in using the extensometer, it is not ideal, as it made grooves or indents on the test specimen since this material is very soft. The load versus displacement curve was obtained on an X–Y plotter. One of the resulting curves is shown in Fig. 8. The average Young's modulus is calculated to be 1.0 GPa and the flow stress to be about 4.5 MPa. It can be seen in the load versus displacement curve that this material shows some plasticity (in compression) before fracturing. If the samples were tested in tension they might well fracture before yielding, as most very brittle materials do. The fracture in the compression samples mostly occurred as a result of spherulitic fiber separation along the specimen load axis.

7. Microhardness

Micro-indentation properties were measured using

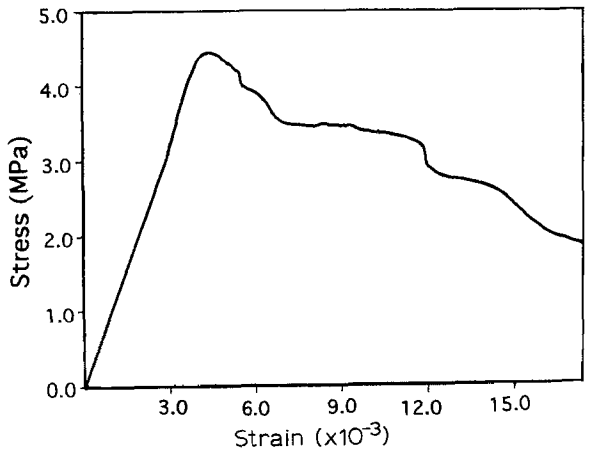

Figure 8 Stress–strain curve for a cholesterol stone tested in compression.

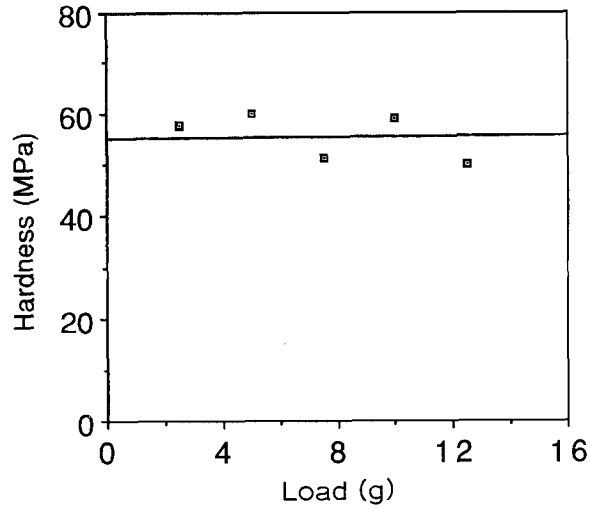

Figure 9 Hardness is plotted versus applied load for a micro-hardness testing machine.

a commercial microhardness testing machine. The Vickers indenter was used for this purpose with a load range of 2–15 g. The hardness was calculated by dividing the indenter load in N by the area of the impression in m^2. Fig. 9 shows the hardness versus the applied load; n.b. that an "ideal" hardness should be totally independent of the load. The hardness for our material is almost constant between 50 MPa and 60 MPa. These values compare well with hardness measurements on cholesterol rich gallstones [14]. It shows that cholesterol is an extremely soft material. At higher loads, the indenter penetrates so deeply into the sample that the resulting impression is disfigured and the size of the diamond pyramid is exceeded. Therefore, micro-indentation techniques with a conventional Vickers diamond could not be used to determine the fracture toughness, as no cracking occurred with small loads and the impressions with large loads are very irregular.

8. Wave speed measurements

The elastic constants were determined using wave speed measurements in the cholesterol samples. Samples were prepared by casting into the shape of a disc of diameter 25.4 mm and thickness 6.39 mm. Both the longitudinal wave speeds, V_p, and the shear wave speeds, V_s, were measured with transducers. A transducer typically incorporates a piezoelectric component, which converts electric signals into mechanical vibration in the generation mode, and uses the inverse effect for signal detection. The sample is held in contact between an emitting and a receiving transducer using coupling gel. Wave speed is measured using pulse echo techniques. In this method, the signal emitted by the transducer undergoes multiple reflections at the free interface. The receiver picks up these signals, which are finally displayed on an oscilloscope. The time measured between two successive reflections is the time taken by the ultrasonic waves to travel twice the thickness of the sample. Thus, by knowing the thickness of the sample and recording these times, we can determine the wave speed in these samples.

The elastic constants and the Poisson's ratio, ν, can be calculated using the following equations [15].

$$\lambda + 2\mu = \rho V_p^2 \tag{1}$$

$$\mu = \rho V_s^2 \tag{2}$$

where λ and μ are Lame's constants and ρ is the density of the material, which is equal to 1.07 g cm^{-3}. Poisson's ratio, ν, is given by

$$\nu = \frac{\lambda}{2(\lambda + \mu)} \tag{3}$$

and Young's modulus, E is

$$E = 2(1 + \nu)\mu \tag{4}$$

The longitudinal wave speed was measured as 1825 m s^{-1} and the shear wave speed was 998 m s^{-1}. From these values Poisson's ratio, ν, was calculated to be 0.28 and Young's modulus, E, to be 2.57 GPa. The shear modulus, μ, is given directly by Equation 2 and is equal to 1.0 GPa. However, this value of Young's modulus is larger than the value we obtained on the universal testing machine. Such differences possibly result from orientation effects between the two samples. In the latter case the spherulitic fibers were running almost parallel to the axial length of the sample, whereas in the wave speed experiments the moduli were measured across the length of the fibers. Furthermore, the value of strain is relatively difficult to obtain for such a fragile material without having an extensometer that is non-contacting to the specimen.

9. Conclusions

Synthetic gallstones grown from the melt or from solution have spherulitic micro structural features very similar to natural gallstones grown *in vivo*. In most cases we have observed the microstructures as being comprised of a single spherulite. The synthetic stones grown from a cholesterol melt exhibit undercooling, characteristic of spherulitic crystallization. The growth kinetics and crystal morphology are a direct result of spherulitic behavior. The radial growth rate is a linear function of time. The growth rate has

been observed as a function of recrystallization temperature. We have suggested a technique to grow synthetic gallstones from cholesterol. Mechanical characterization of these synthetic stones shows that they are very soft and ductile materials, but they are still very brittle and contain large cracks. We have obtained stress–strain curves that show yielding at about 5 MPa for the synthetic cholesterol stones made in cast molds.

Acknowledgements

We would like to thank Mr A. K. Agarwal for his help with the DSC work, Mr G. S. Dahake for his help in wave speed measurements and Dr K. L. Marshall for assisting with the hot stage microscopy. This work was supported by the National Institutes of Health through USPHS Grant No. DK 39796.

References

1. D. J. SUTOR and S. E. WOOLEY, *Gut* **12** (1971) 55.
2. P. M. BILLS and D. LEWIS, *ibid.* **16** (1975) 630.
3. D. J. SUTOR and S. E. WOOLEY, *ibid.* **15** (1974) 487.
4. N. H. AFDHAL and B. F. SMITH, *Hepatology* **11** (1990) 701.
5. G. M. MURPHY, *J. Phys. D Appl Phys.* **24** (1991) 119.
6. J. M. BEENS, P. M. BILLS and D. LEWIS, *Gastroenterology* **76** (1979) 548.
7. "CRC handbook of chemistry and physics" (CRC press, 1991–1992) p. 3.
8. H. D. KEITH and F. J. PADDEN, Jr, *J. Appl. Phys.* **34** (1963) 2409.
9. J. SCHULTZ, "Polymer material science" (Prentice Hall, New Jersey, 1974) p. 181.
10. S. J. BURNS, S. M. GRACEWSKI, N. VAKIL and A. R. BASU, in "Dynamic failure of materials: theory, experiments and numerics", edited by H. P. Rossmanith and A. J. Rosakis (Elsevier Applied Science, New York, NY, 1991) p. 114.
11. J. H. MAGILL, *J. Appl. Phys.* **35** (1964) 3249.
12. H. D. KEITH and F. J. PADDEN, Jr, *ibid.* **35** (1964) 1286.
13. S. J. SCHULTE and R. L. BARON, *American Journal of Roentgenology* **155** (1990) 1211.
14. S. M. GRACEWSKI, N. VAKIL, E. C. EVERBACH, M. E. DAVIS and S. J. BURNS, *J. Mater. Sci. Lett.* **11** (1992) 554.
15. H. KOLSKY, "Stress waves in solids" (Dover Publications, New York, NY, 1963) Ch. 2.

Received 12 January
and accepted 15 January 1993